A Method for Evaluating Power System Security Region under Uncertainties and Its Application to Transient Stability Problem

Naoto Yorino, Yuki Nakamura, Muhammad Abdillah, Yutaka Sasaki, Yoshiharu Okumoto
Graduate School of Engineering
Hiroshima University
Higashi-Hiroshima, Japan
yorino@hiroshima-u.ac.jp

***Abstract*—Due to rapid expansions of renewable energy (RE) generations, it becomes more important to assess the feasibility of power system operation under limited controllable resources. Especially, exact evaluation of the system reserve for preserving system security is required under erroneous RE output predictions. This paper proposes a new method to evaluate the existence of the feasible region under uncertainties. Predicted RE and demands with their confidence intervals (CIs) are specified to formulate a problem for the evaluation of the size of the worst-case feasible region, where positive size implies feasibility, while negative, infeasibility. The method computes the degree of system security for the worst case, which is referred to as "Robust Power System Security" in this paper. The problem is formulated as bi-level optimization, which is linearized and transformed into the mixed integer linear programming (MILP) problem. This is a new approach in the treatment of uncertainties. We use a linear constrained dynamic economic dispatch problem to demonstrate the effectiveness of the proposed method. The latter half of the paper focuses on transient stability (TS) problem. We show that there may exist various critical patterns of uncertain power flows due to photovoltaic (PV) generations in West Japan System. We propose the use of critical clearing time (CCT) as a TS index, which is effectively computed by means of the critical trajectory (CTrj) method. We also suggest a distribution factor (DisF) to control CCT, which is referred to as CCT-DisF in this paper. Then, the proposed worst-case optimization method is applied to the TS control problem to develop a robust security monitoring and control method under uncertain PV generations.**

Keywords—Power system security, power system reliability, generator's operation regions, probabilistic security assessment, deterministic security assessment.

NOMENCLATURE

Variables and Functions:

d	Diameter of upper and lower bounds of security region
$f^n(*)$	Power flow equations (equality constraints)
$g^n(*)$	Inequality constraints in power flow problem
$H(*)$	Power flow constraint set consisting of f^n and g^n *for all n*
$H_{DF}(*)$	Unified constraint set consisting of $H(*)$ and dynamic ramp rate constraints
$p=[P_{PV}, P_D]$	Uncertain parameter vector (uncontrollable)
P_D	Load (MW)
P_G	Output power of generators (MW)
P_{PV}	Output of photovoltaic generations (MW)
P_{slack}	Output of slack node generators (MW)
P_{TL}	Transmission line flow (MW)
$u=[P_G, P_{slack}]$	Control vector (node injection by generators)
x	Dependent variables (voltage vector)
δ	Maximum ramp-rate of generator

Parameters:

c	Normal vector for objective
CD_u	CCT distribution factor with respect to u
e	Unit vector
n	Contingency number ($n = 0$ for normal condition, $n = 1, ..., N$ for contingencies)
N_B	The number of nodes
$\hat{p}(t \mid t_0)$	Estimation of p at t predicted at t_0
$S^{(n)}$	Transformation matrix from node injection to line flow for contingency n (DC power flow)
t	Time point (t_0: base point, $t_0 < t$: future point)
$\overline{\Delta}(t \mid t_0)$	Maximum prediction error
$\overline{\Delta}_D(t \mid t_0)$	Maximum error for load forecast
$\overline{\Delta}_{PV}(t \mid t_0)$	Maximum error for PV forecast
$\overline{*}$, $\underline{*}$	Upper and lower bounds of variables $*$

Regions and Sets:

DF_u	Dynamic feasible region (Set of u)
R_p	Region of uncertain parameter p (Set of p)
RDF_u	Robust dynamic feasible region (Set of u)
RSS_u	Robust static security region (Set of u)
SS_u	Static security region in u space (Set of u)

Abbreviation:

CCT	Critical Clearing Time
CTrj	Critical Trajectory
CI	Confidence interval
CL	Confidence level
CPU	Central processing unit

DisF	Distribution Factor
LB	Lower bound
MILP	Mixed integer linear programming
PV	Photovoltaic
RE	Renewable energy
TS	Transient Stability
UB	Upper bound

I. Introduction

The development of RE technology is a solution of world energy problems, while the recent expansion of RE is causing difficulties in electric power system operations. In Japan, especially PV generation is rapidly increasing and threatening the grid security as well as power quality. Treatment of PV output uncertainty is a key subject in power system planning and operations.

So far the N-1 security criterion has been used worldwide to maintain power system security and reliability [1]-[3]. The criterion is widely used in various practical methods [4]-[6]. Various studies on the system security issue have been performed related to contingency analyses. The worst-case computation based on the bi-level optimizations for disruptive threat [7], [8], interdiction [9], vulnerability analysis [10], contingency ranking [11]. Contingency constrained power system optimizations have been proposed such as for optimal power flow [12], [13], unit commitment problem [14], transmission expansion [15] and FACTS allocation problem [16].

On the other hand, since various problems arise in power system planning and operations due to rapid increase in REs, various trials and methods have been proposed to take into account their uncertainties effectively. Those researches include robust optimization for unit commitment and economic dispatch [17], [18], the computation of cautious operation planning and worst case scenario [19], [20], decision-making process [21], and stochastic security constraint unit commitment using energy storage system [22].

While such various approaches are being developed, the increase in uncertainties is being accelerated. Therefore, more direct assessment of the feasibility of system operations is being required. Power system flexibility is becoming an important subject in the evaluation of the maximum ranges of uncertainties without deteriorating power system reliability [23]-[25]. Using this concept, the maximum ranges for REs are computed as do-not-exceed limit [26], [27]. There are more direct evaluation of feasible region under uncertainties, such as the evaluations of dispatchable region of variable wind generation [28] and of loadability sets [29].

We have defined and used a term “Robust Power System Security” implying the robustness of maintaining the power system security criterion for all pre-specified uncertainty set [30], [31], where we analyze TS to alert future power system operations in Japan. We developed a direct method for the computation of CCT for TS problem in [32]-[34], which has been improved so far. The basic concept of Robust Power System Security is that the uncertain events and disturbances may be divided into “acceptable” and “unacceptable” categories. In the former case, the impact is small enough that the system can be recovered within assumed payable cost; probabilistic methods are suited for this case such as cost minimizations. The latter events may result in fatal consequences such as blackout, which must be avoided even if the probability is small. Based on this idea we have defined the robust security region as the feasibility region by the important constraints for the latter case in [35], where an approximate solution is also proposed. The basic idea is similar to the flexibility in [23]-[27], while the main difference is that, instead of computing the maximum ranges of uncertainties, we measure the operational feasibility in the space of control variables for the pre-specified uncertainty set. We have developed a real-time unit commitment and economic dispatch method in [36] where transmission over loadings are treated by stochastic power flow while supply demand balance is guaranteed by the computation of feasibility region [37], [38] for the maximum prediction errors and contingencies.

In this paper, we extend our previous works on “Robust Power System Security” in [30], [31], [35] and formulate a bi-level optimization problem for evaluating the worst-case feasibility of power system operation under uncertainties. The contributions of this paper are given as follows:

1. We present a novel formulation and method to compute the size of the feasible region under dynamically varying prediction errors in system operation.
2. The method is useful to assess Robust Power System Security guaranteeing the security criterion, which is applied to the dynamic economic dispatching problem using DC power flow model.
3. By selecting operation cost as objective function, the method can evaluate the worst-case economic operation planning, while measuring the size of feasibility region including infeasible cases.

In the latter half, we study TS problem. We show that there may exist various critical patterns of uncertain power flows due to photovoltaic (PV) generations in West Japan System. Then, we propose a monitoring and control method of TS as an application of the robust power system security approach as below:

4. We propose a CCT based TS analysis method. We show that CCT is an effective index for monitoring and control of TS when combined with CTrj method. We also propose CCT-DisF for preventive control of TS.
5. We formulate a CCT based Bi-level optimization method to enhance TS in real time operation under uncertainty.

The rest of the paper is organized as follows. Robust Power System Security regions are explained in Section II. Formulation for network security assessment is described in Section III. Application to dynamic economic dispatch problem is illustrated in Section IV. TS in West Japan System

is analyzed using CCT in section V. CCT-DisF and a preventive control method for TS are presented in section VI. Robust security control method is proposed in section VII. Conclusion is given in Section VIII.

II. Robust Power System Security Regions

A. Conventional Security Criterion

In this section, the conventional deterministic security criterion such as N-k criterion is represented by a set of constraints in order to be extended to a new criterion. First, we express the power flow equations and constraints before and after contingencies as follows.

$$\left.\begin{aligned} &\boldsymbol{f}^n(\boldsymbol{x},\boldsymbol{u},\boldsymbol{p})=0\,,\ \boldsymbol{g}^n(\boldsymbol{x},\boldsymbol{u},\boldsymbol{p})\le 0 \\ &\boldsymbol{f}^n:\mathbb{R}^{B+G+L}\to\mathbb{R}^B,\ \underline{\boldsymbol{u}}\le\boldsymbol{u}\le\overline{\boldsymbol{u}}, \\ &\boldsymbol{x}\in\mathbb{R}^B,\ \boldsymbol{u}\in\mathbb{R}^G,\ \boldsymbol{p}\in\mathbb{R}^L, n=0,1,\cdots,N \end{aligned}\right\} \tag{1}$$

The problem consists independent conditions with n=0~N, where n=0 represents pre-fault condition and n=1~N stands for N post-fault contingency conditions to define the conventional deterministic security criterion including N-k criterion. In system operation planning, while p is predicted, control u matching load p is determined to satisfy the constraints. We suppose that (u, p) does not change before and after the fault when studying static problem, which will be extended to dynamic problem in the latter section. The conventional deterministic security criterion implies that an operating point (u, p) satisfies (1).

B. Static Security (SS) Region Satisfying Security Criterion

Given load p, the feasible region of control variable u satisfying all the constraints (1) is defined as:

$$\left.\begin{aligned} &SS_u(p)=\left\{u\,|\,SS_u^0(p)\cap SS_u^1(p)\cap\cdots\cap SS_u^N(p)\right\} \\ &SS_u^n(p)=\left\{u\,|\,\underline{u}\le u\le\overline{u},\ f^n=0,\ g^n\le 0\right\} \\ &n=0,1,\cdots,N \end{aligned}\right\} \tag{2}$$

Or, an equivalent representation is:

$$SS_u(p)=\left\{u\,|\,H(x,u,p)\le 0\right\} \tag{3}$$

H is the constraint set included in (1) and (2), which define a region of u. We call the region "Static Security (SS) region" defined for a snapshot of power system operation at specific time. SS region is the region of generator outputs satisfying the conventional security criterion for specific parameter values of p. Power system operating point inside SS region is equivalent to that the system state is secure based on the security criterion.

C. Dynamic Feasible (DF) Region

Generators have dynamic operation constraints such as output power change rate limitation due to thermal stress. The controllable generator outputs at two time points t_0 and t are restricted by maximum ramp-rate δ per unit time.

$$-\delta\cdot(t-t_0)\le u(t)-u(t_0)\le\delta\cdot(t-t_0) \tag{4}$$

Therefore, given an initial operating point $u(t_0)$ at t_0, we may define a security region at each time t, reachable from the initial point. The region is referred to as DF region in this paper defined by the set of time points $u(t_1)$, $u(t_2)$, .., $u(t)$ satisfying constraints (3) and (4) for all t, ($t_0<t$). Where t_0 represents the current time or initial time point under study and each time point t_1, t_2, t_3 ... represents future time points.

DF region is represented as

$$\begin{aligned} &DF_{u(t)}(p(t)) \\ &=\left\{u(t)\,|\,H_{DF}(x(t),u(t),p(t))\le 0,\ \text{given}\,u(t_0)\right\} \end{aligned} \tag{5}$$

H_{DF} is the constraint set consisting of (3) and (4) for all t, ($t_0<t$).

D. Robust Static Security (RSS) Region with Uncertainties

In this section, we consider the power system security in the presence of uncertainties in parameter vector p. We first assume a simple case of uncertainties bounded in the following form.

$$R_P=\{p\,|\,\underline{p}\le p\le\overline{p}\} \tag{6}$$

$\overline{p}$, $\underline{p}$: upper and lower bounds of uncontrollable variable p.

RSS region is defined as the safe-side security region for all possible parameter variations as follows:

$$\begin{aligned} RSS_u&=\left\{u\,|\,u\in\bigcap_{p\in R_p}SS_u(p)\right\} \\ &=\left\{u\,|\,H(x,u,p)\le 0\ \text{, for all}\ p\in R_p\right\} \end{aligned} \tag{7}$$

E. Robust Dynamic Feasible (RDF) Region

Estimation of fluctuation parameter such as load forecast is very important for power system operation. Expressing $p(t)$ for such a fluctuation parameter vector at time t, we assume the following form of estimation formula.

$$\begin{aligned} &p(t)=\hat{p}(t\,|\,t_0)+\Delta(t\,|\,t_0) \\ &\Pr\{\underline{p}(t)\le p(t)\le\overline{p}(t)\}=CL,\quad 0\le CL\le 1 \end{aligned} \tag{8}$$

Here, the first term in (8) is the forecast $\hat{p}(t\,|\,t_0)$ of $p(t)$ predicted at t_0, and the second term is the prediction error $\Delta(t\,|\,t_0)$, which corresponds to "uncertainty" in this paper. The uncertainty is characterized by the confidence interval, CI, upper and lower bounds with confidence level, CL. The uncertainty usually becomes larger as forecast time $t-t_0$ increases. In this paper, we will take a standpoint that CL is specified so that the bounds of uncertainties as well as

parameters are determined. Confidence intervals of $p(t)$ at time t is defined as follows.

$$R_{p(t)} = \{p(t) \mid \underline{p}(t) \le p(t) \le \overline{p}(t)\}$$
$$\underline{p}(t) = \hat{p}(t \mid t_0) + \underline{\Delta}(t \mid t_0),\ \overline{p}(t) = \hat{p}(t \mid t_0) + \overline{\Delta}(t \mid t_0) \quad (9)$$

The expression permits uncertainty Δ around prediction $\hat{p}$ for selective value of CL. Practically, maximum forecast error in p may be identified as bounds of Δ. An example is given in Fig. 1. The time to carry out the prediction will be at some future point ($t = t_0$) such as at 24 hours before the real time operation. In this situation, the accuracy of prediction errors is available in advance and reasonable values of the maximum errors can be set for each prediction time based on the historical data analysis. In the proposed method, we use the confidence interval for this setting [36] in order to obtain the reliable result. In the latter section, we use the following form for the bounds of uncertainties.

$$\underline{\Delta}(t \mid t_0) = -\sigma \cdot (t - t_0),\ \overline{\Delta}(t \mid t_0) = \sigma \cdot (t - t_0) \quad (10)$$

This implies that uncertainties are nonexistence at $t = t_0$ and increase with respect to t for future predictions. Power system planning and operation task are usually based on four stages, which are yearly system planning (reinforcement planning, expansion planning), electric power demand-supply planning from monthly to weekly, day ahead operation planning, and real-time operation.

For each stage, we examine power system security. In the conventional power system operations, p of load power is almost patterned and rather easily forecasted, where uncertainties are small. However, as RE is largely penetrated, the outputs may be fluctuated due to weather condition causing larger forecast error and then the power system planning and operation tasks should consider directly Δ of uncertainties.

Robust Dynamic Feasible (RDF) Region is defined as

$$RDF_{u(t)} = \{u(t) \mid u(t) \in \bigcap_{p \in R_{p(t)}} DF_{u(t)}(p(t))\}$$
$$= \{u(t) \mid H_{DF}(x(t), u(t), p(t)) \le 0, \quad \text{for all } p(t) \in R_{p(t)}, \text{ given } u(t_0)\} \quad (11)$$

In [30], [31], [35], further definition is given for Robust Dynamic Security (RDS) region taking into account dynamic characteristics of power system transitions. The concept of the regions for robust security is shown in Fig. 2.

The next problem is the computation of the regions sizes of RSS and RDF. The region sizes can be very important security measure for the power system operation against uncertainties.

III. Formulation for Network Security Assessment

A. Measure of SS Region Size

In order to measure the size of SS region, we use the following hyper-plane with a pre-specified normal vector, c [35].

$$c^T u = \alpha \quad (12)$$

When parameter α varies, there exit intersection of the SS region and hyper-plane if SS region exists. The region of α for the existence of the intersection is represented as follows.

$$\underline{\alpha}_{SS(p)} \le \alpha \le \overline{\alpha}_{SS(p)} \quad (13)$$

The concept is described by Fig. 3. Then, we propose the following problem formulation to obtain the upper (UB) and lower (LB) bounds respectively as:

$$\text{(UB)} \quad \overline{\alpha}_{SS(p)} =: \max_u c^T u \quad (14)$$

Subject to $H(x, u, p) \le 0$ with given p.

$$\text{(LB)} \quad \underline{\alpha}_{SS(p)} =: \min_u c^T u \quad (15)$$

Subject to $H(x, u, p) \le 0$ with given p.

B. Region Size Problem for RSS

In this section, we propose a method to calculate the upper and lower bounds of α for RSS region taking into account uncertainties.

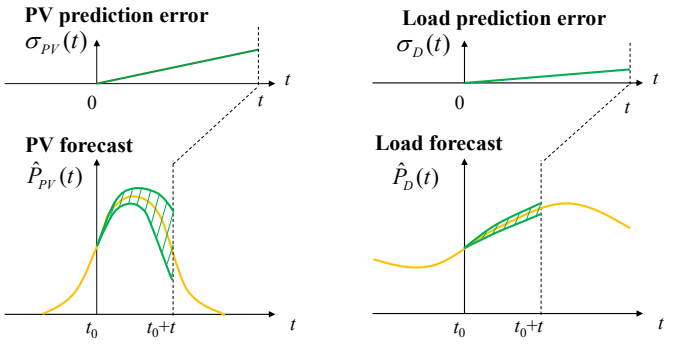

Fig. 1. Setting for PV and Load situations.

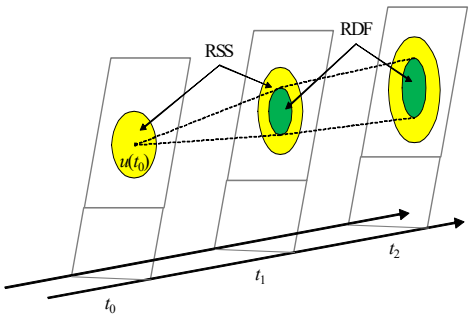

Fig. 2. Concept of robust security regions.

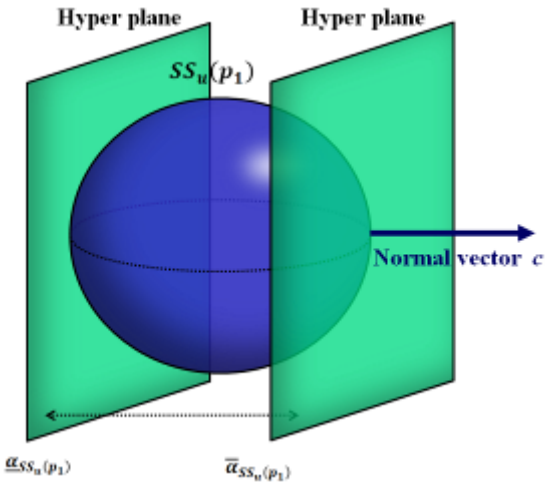

Fig. 3. Measure of SS region size using hyper-planes.

$$\underline{\alpha}_{RSS} \le \alpha \le \overline{\alpha}_{RSS} \tag{16}$$

First, $\overline{\alpha}_{RSS}$ corresponds to the lower bound of $\overline{\alpha}_{SS(p)}$ for all possible parameter values of p in CI, and therefore, it may be represented as the following condition.

$$\overline{\alpha}_{RSS} = \min_{p \in Rp} \overline{\alpha}_{SS(p)} \tag{17}$$

Therefore, by extending the formulation for SS region, the RSS may be formulated as a bi-level optimization problem.

$$\text{(UB)} \quad \overline{\alpha}_{RSS} =: \min_{p \in Rp} \{ c^T u \} \tag{18}$$

Subject to $H(x,u,p) \le 0$.

$u \in \arg\max_u \{c^T u\}$

Subject to $H(x,u,p) \le 0$.

$$\text{(LB)} \quad \underline{\alpha}_{RSS} =: \max_{p \in Rp} c^T u \tag{19}$$

Subject to $H(x,u,p) \le 0$.

$u \in \arg\min_u \{c^T u\}$

Subject to $H(x,u,p) \le 0$.

Fig. 4 shows the deviation of the upper and the lower bounds of SS region when p is varied, in which the lowest upper bound and the highest lower bound define the bounds of RSS region with respect to normal direction c.

The distance d between the bounds may be a useful index expressing the RSS region size for the direction of vector c.

$$d = \frac{1}{\| c \|} (\overline{\alpha}_{RSS} - \underline{\alpha}_{RSS}) \tag{20}$$

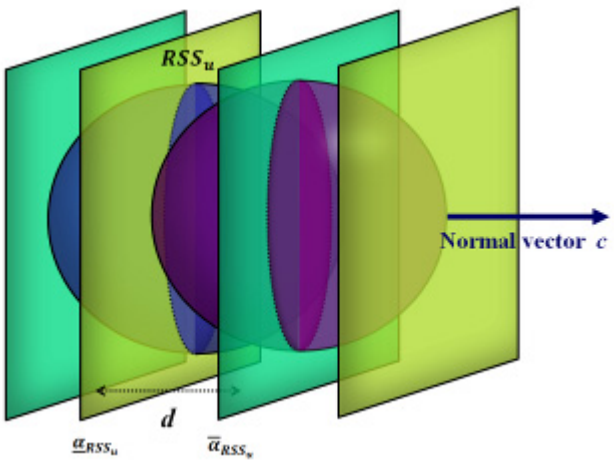

Fig. 4. Measure of RSS size for deviations of SS region

Index d is positive when RSS is existence and its absolute value represents the region size, while it is negative when RSS is nonexistence. The larger the index, the system is able to be operated more easily inside the RSS region where the system security is preserved. By setting different direction c, the length of RSS for the different direction may be obtained.

When the volume of RSS becomes small, d always indicates small value except when choosing a very special direction c. Furthermore, d always becomes negative without exception when the volume of the intersection disappears.

We recommend that it is better to avoid the system operation on the edge of the security region RSS. However, the worst thing is that no security region exists where d shows a negative value. In this case, we need some action to keep or enlarge the region for increasing d in order to keep operating point inside the security region. This is easily carried out as we will demonstrate in section IV.D.

C. Region Size Problem for RDF

The proposed formulation for RSS is easily extended to the case for RDF. The problem is translated into discrete time point sequence, t=0, 1, 2, … with given initial point $u(0)$. The region size problem for RDF may be formulated as follows.

$$\text{(UB at } t\text{)} \quad \overline{\alpha}_{RDF}(t) =: \min_{p(t)} \{ c^T u(t) \} \tag{21}$$

Subject to $H_{DF}(x(t),u(t),p(t)) \le 0$,

$u(t) \le u(t-1) * + \delta$

$\underline{p}(t) \le p(t) \le \overline{p}(t)$

$u(t) \in \arg\max_u \{c^T u(t)\}$

Subject to $H_{DF}(x,u,p) \le 0$

$u(t) \le u(t-1) * + \delta$

$\underline{p}(t) \le p(t) \le \overline{p}(t)$.

With given $u(0)$, present operating point.

$u(t-1)^*$ is solution of (UB at t-1)

The solution of the problem is sequentially obtained from t=1, 2, 3, … The lower bound problem is formulated in the same way as follows:

$$\text{(LB at } t\text{)} \quad \underline{\alpha}_{RDF}(t) =: \max_{p(t)} \{ c^T u(t) \} \tag{22}$$

$$\text{Subject to} \quad H_{DF}(x(t), u(t), p(t)) \le 0,$$

$$u(t) \ge u(t-1)^{**} - \delta$$

$$\underline{p}(t) \le p(t) \le \overline{p}(t)$$

$$u(t) \in \arg\min_{u} \{ c^T u(t) \}$$

$$\text{Subject to} \quad H_{DF}(x, u, p) \le 0$$

$$u(t) \ge u(t-1)^{**} - \delta .$$

$$\underline{p}(t) \le p(t) \le \overline{p}(t)$$

With given $u(0)$, present operating point.

$u(t-1)^{**}$ is solution of (LB at t-1)

Index d may be computed in the same way as Equation (20) to effectively evaluate the reliability of the power system operations.

In common with RSS and RDF, the fluctuation of security region by the uncertainty affect the diameter of security region as depicted in Fig. 4. It can be stated that when the forecast is very exact the security region does not fluctuate and keep large size, where d also is large. In this situation, it is guaranteed that the operator can easily control the operating point inside the security region under all possible situations with uncertainties. Therefore, the system operation can be reliable and secure.

D. Solution Method

The problems formulated based on bi-level optimization framework in the previous section may be solved by the combination of successive linearization and transformation into mixed integer linear programming (MILP). The solution is obtained by the following steps.

Step 1: Linearize (21) and (22) to obtain (A.1)-(A.4).
Step 2: Transform them into MILP problems (A.5)-(A.11)
Step 3: Solve the MILP problems to obtain solutions.

If necessary, repeat the process based on the successive linearization method although we focus on only a linear problem in this paper in the next section. Note that the transformation into the MILP problem in step 2 is given in the Appendix.

IV. Application to Dynamic Economic Dispatch Problem

A. Outline of Examinations

In this section, we demonstrate possible applications of proposed method in the economic dispatch problem. As illustrated in Fig. 2, when a present operating point is given at t_0, the feasibility of the future operating points depends on the capability of the system, future system conditions and uncertainties. Namely, when we obtain the future predictions and maximum prediction errors available at t_0, we can evaluate the reliability of future system operations from the maximum dynamic performance of the system. This is exactly the robust security analysis proposed in this paper. We demonstrate examples of security assessment of future 24 hours operating conditions, given an operating point at t_0. We assume a situation where load forecast and PV output forecast for 24 hours and their maximum errors are available at t_0.

B. Dynamic Generation Dispatch Model

We study a linearized dynamic economic dispatch problem in the form of (21) and (22). In general, there may exist controllable generators and uncontrollable loads and PVs in the individual nodes. Then, we assume that the node injections consist of controllable and uncontrollable variables as follows:

Node Injection: $u + p, \quad u \in R^{N_B}, p \in R^{N_B}$

We use a well-known and widely used model for static economic dispatch problem.

Supply & Demand balance: $e^T \cdot (u + p) = 0$ (23)

Line Flow Limit: $\underline{P}_{TL} \le S^{(n)} \cdot (u + p) \le \overline{P}_{TL} \quad n = 1 \ldots N$ (24)

Controllable generator limits: $\underline{u} \le u \le \overline{u}$ (25)

$R_p = \{ p \mid \underline{p} \le p \le \overline{p} \}, \; p = [P_{PV}, P_D]$ (26)

The above equations correspond to linear version of H in (3), where, $e = [11 \ldots 1]^T$. Equation (24) may work as security limits. R_p in equation (26) implies the region that the uncertain parameters exist as is exemplified by the shaded areas in Fig.1. In addition to the above static constraints, the ramp rate constraint is taken into account in the dynamic economic dispatch model of H_{DF} in (21) and (22).

$$-\delta \le u(t+1) - u(t) \le \delta \tag{27}$$

C. Uncertainty Model

We assume uncertainties in the form of (6) for PV generations and load consumptions. We fully utilize load forecast and PV output forecast for 24 hours (t=1, 2,…, 24) at t=0, present operating time. In this situation, we assume that the upper and lower limits of the prediction errors are given by.

$$-\underline{\Delta}_{PV}(t \mid t_0) = \overline{\Delta}_{PV}(t \mid t_0) = \sigma_{PV} \cdot (t - t_0) \cdot \hat{P}_{PV}(t \mid t_0) \tag{28}$$

$$-\underline{\Delta}_{D}(t \mid t_0) = \overline{\Delta}_{D}(t \mid t_0) = \sigma_{D} \cdot (t - t_0) \cdot \hat{P}_{D}(t \mid t_0) \tag{29}$$

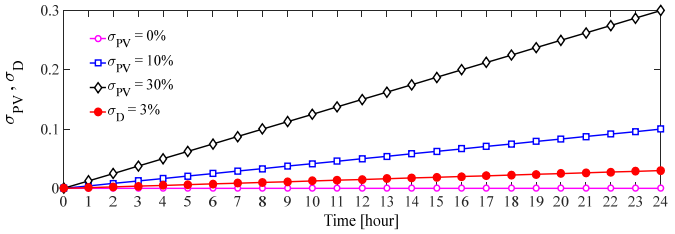

Fig. 5. Maximum prediction error $\sigma(t)$.

Where $\overline{\Delta}_{PV}(t\,|\,t_0), \underline{\Delta}_{PV}(t\,|\,t_0), \overline{\Delta}_D(t), \underline{\Delta}_D(t)$: upper and lower bounds of PV and load prediction errors for 24 hours (t=1, 2,…,24) which are evaluated at t_0. Coefficients $\sigma_{PV}(t)$, $\sigma_D(t)$ represent prediction accuracies. The equations imply that the prediction errors increase for more future forecast as given in Figs. 1 and 5.

In the simulations in the following sections, we set three cases of PV forecast: $\sigma_{PV}(t)$ = 0% (non-uncertainty), 10%, 30% (higher uncertainty), which imply maximum PV prediction errors of 24-hour ahead. Meanwhile, $\sigma_D(t)$ is set to 3% for maximum error of load forecast.

D. Remarks

In summary, the maximization problem is expressed by objective (21) with constraints (23) to (27). The decision variables are u and p for t=1...24. Inputs are their upper and lower bounds, while outputs are the optimal u for the worst case of p inside the bound pre-specified by (28) and (29). The minimization is the same except for objective (22). After the optimizations, d is obtained. If d is too small, we can find possible actions to increase d by relaxing the active constraints given also by the results of the optimizations. The actions include additional power supply at the constrained node, demand response, curtailment of PV output, load shedding, etc.

We can analyze different problems by selecting the normal vector $c = [c_1 c_2 \cdots c_{NB}]^T$ in the objective as follows.

1) Production cost setting:

When the generator cost coefficients are set, the lower bound solution implies the worst case economic operating point against uncertainties, while d indicate the size of feasibility region measured in MW. The solution with positive d guarantees the secure power system operation.

2) Total power supply setting:

By setting c_i = 1 for generators, and 0 for slack and other buses, the objective corresponds to the total generation.

$$cu = \sum_{i \in GeneratorBus} u_i \qquad (30)$$

This case directly analyzes the adequacy of total power supply.

E. Numerical Examples of Feasibility Region

The proposed method is illustrated using 3-generator model

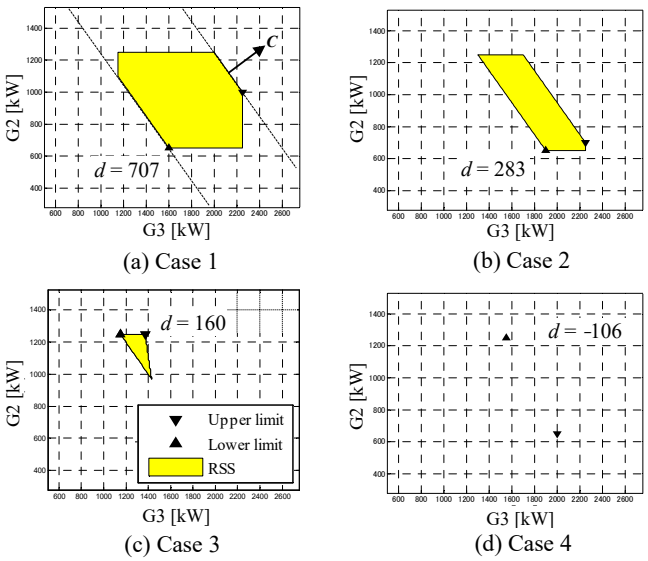

Fig. 6. RSS region in G_2-G_3 output space.

cited from our previous work in [35]. We only describe the results of computation to confirm the validity and the accuracy of the proposed method. Figs. 6 (a)-(d) show the feasibility regions (RSS) for different sizes of uncertainties. The region shrinks as the uncertainty increases. The triangle points indicate the upper and lower bounds computed by the proposed method, which provides the region size accurately.

F. 6-Bus System Example

A six-bus test system illustrated in Fig. 7 is used in this section to demonstrate 24-hour Robust Security Assessment based on the proposed method. The system data are cited from [40], [41], including ramp-rate data and the daily total load

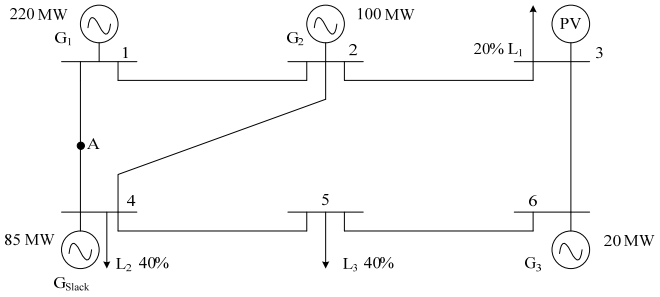

Fig. 7. Six-bus test system.

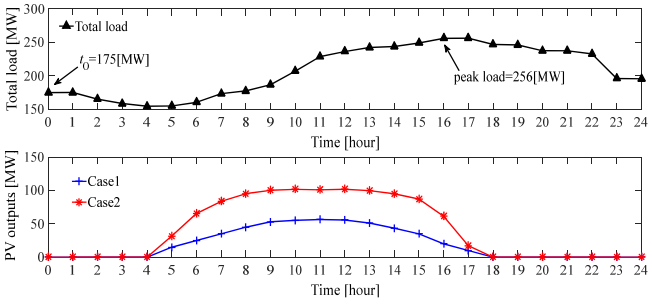

Fig. 8. Daily load and PV curves.

data given in Fig. 8.

The slack generator capacity (85MW) and PV generation unit are added at buses 4 and 3, respectively. Then, the system has four controllable generators, and uncontrollable three loads and one PV generation unit.

We use daily PV data from the 2006 National Renewable Energy Laboratory Dataset [42]. In order to analyze the robustness of the proposed method, we set two cases as follows,

Case 1: PV capacity is 74MW (28.9% of peak load 256MW).
Case 2: PV capacity is 125MW (48.8% of peak load 256MW).

The daily PV data for sunny day is depicted in Fig. 8.

As a contingency, single line outage of double circut lines is assumed at point A between buses 1 and 4 in Fig. 7.

First, a conventional static economic dispatch method is used to determine the operating point at t_0. We use the original system data, that is, the total load at t_0 is 175MW with load distribution 20% at bus 3, 40% at buses 4 and 5, which are varied proportionally with time.

Next, we solve the proposed problems to calculate the $\underline{\alpha}_{RDF}, \overline{\alpha}_{RDF}$ with the production cost setting to obtain Fig. 9. The result corresponds to forecast errors of $\sigma_{PV} = 30\%, \sigma_D = 3\%$ in case 2. For this figure, the abscissa is the time point t at 0, 1, 2, .. , 24 o'clock, where t = 0 is the current time at which the load and PV output predictions are carried out for 24 hours. $\underline{\alpha}_{RDF}$ with the production cost setting implies the recommended secure operation pattern while $\overline{\alpha}_{RDF}$ the upper bound of the feasible region guaranteeing the security criterion. Note that the reverse of $\underline{\alpha}_{RDF}$ and $\overline{\alpha}_{RDF}$ is observed at around 14:00 o'clock. This implies that the operation itself is possible but the operating point is not inside the security region since the region itself disappears.

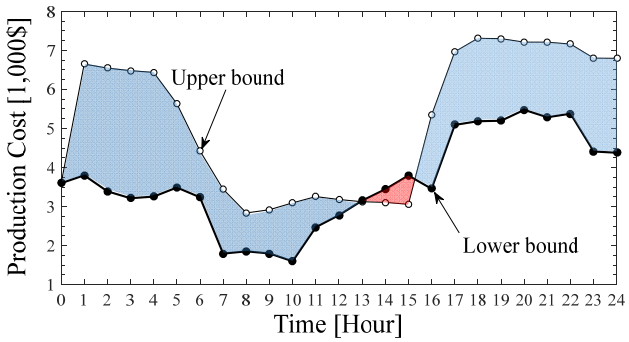

Fig. 9. The bounds of feasibility region with production cost setting; the lower bound indicates the worst case economic operation

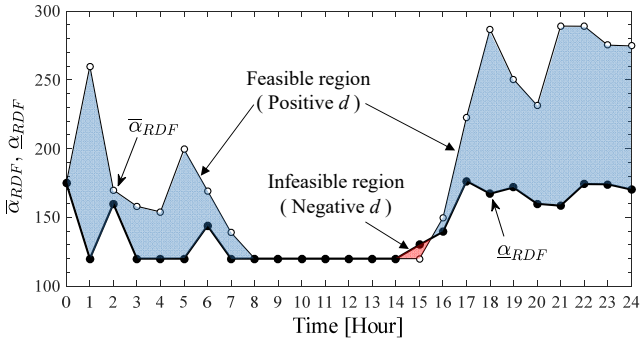

Fig. 10. The bounds of feasibility region with total power supply setting; Reverse of upper and lower bounds indicates infeasibility.

Fig. 10 shows the same computation with the total power supply setting. This setting can directly measure the flexibility of the total power supply. The region between $\underline{\alpha}_{RDF}$ and $\overline{\alpha}_{RDF}$, blue colored area, is the feasible region with positive d. We can observe the same result as before that the system operation is not secure at around 14:00 o'clock with negative d. Demand and supply balance may not be guaranteed in these time periods depending on conditions of PV generations and loads.

As we have observed, distance d is a useful indicator representing the size of the security region, where the system operation is easier for a greater d. Fig. 11 (a)-(d) show indicator d of RDF for different conditions PV forecast. The

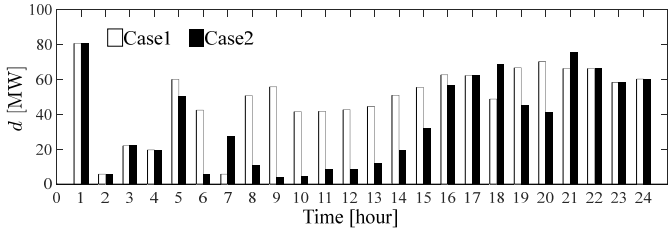

(a) $\sigma_{PV} = 0\%, \sigma_D = 3\%$

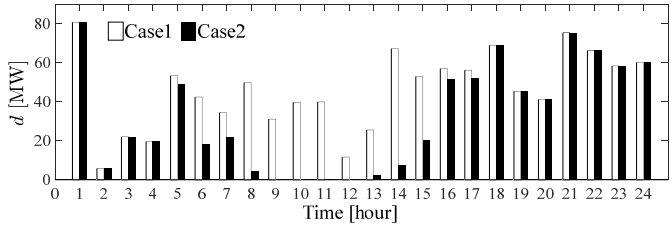

(b) $\sigma_{PV} = 10\%, \sigma_D = 3\%$

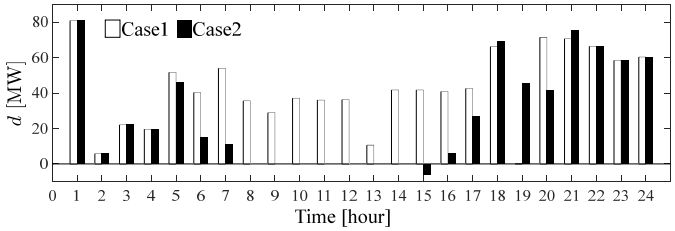

(c) $\sigma_{PV} = 30\%, \sigma_D = 3\%$

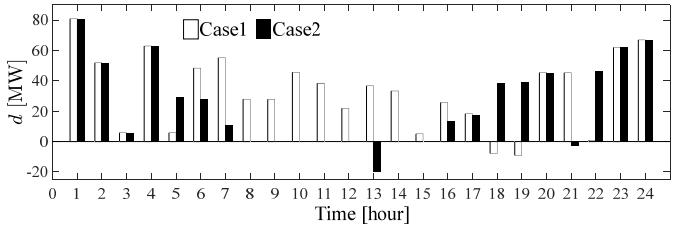

(d) $\sigma_{PV} = 30\%, \sigma_D = 3\%$ and N-1 contingency

Fig. 11. Size of feasibility region d measured in MW; Negative values indicate possible power mismatch in the worst case.

white bars represent d for case 1 and black bars for case 2. When the forecast is very exact, d is large as seen in Fig. 11(a) as expected by theoretical point of view.

When the forecast is degenerated, d tends to become small and sometimes negative, where the robust security cannot be guaranteed as observed in Figs. 11(b), (c) and (d). It is needless to say that the indicator d for case 1 and 2 is equal during night when PV outputs are zero: the distance d shows large values since PV uncertainties are nonexistence.

G. 118-Bus System Example

A modified IEEE 118-bus test system is used to verify the effectiveness of indicator d. The system consists of 54 generators, 186 transmission lines, and 91 loads. The system data are given in [43]. The total load at t_0 is 3733 MW. The peak load is 4080 MW. The daily total load and PV data are shown in Fig. 12(a)-(b). The slack generator is located at bus 30 whose capacity is 1805MW. We set two cases by changing the amount of PV installation capacities to examine the performance of the proposed method as follows:

Case 1: 722 MW PV capacity (17.69% of peak load).
Case 2: 1262 MW PV capacity (30.93% of peak load).

The above PV's are distributed into 5 areas given in Table I.

Fig. 13(a)-(d) depict the distance d between the bounds of RDF for two cases with maximum prediction errors of $\sigma_{PV} = 0\%$, 10%, 30%, and 30% with contingency scenario, respectively. For the contingency case, we assume outage of

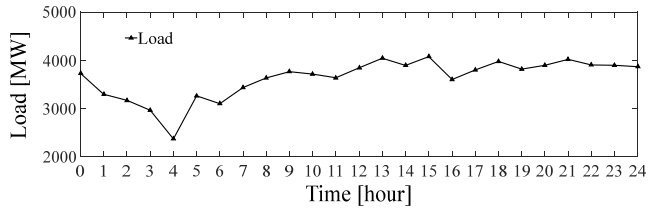

(a) Hourly total load data

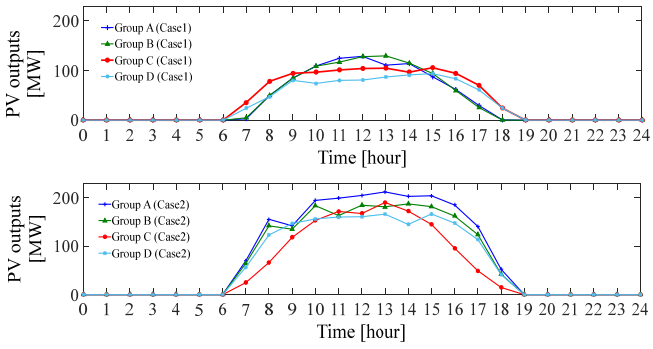

(b) Hourly total PV data

Fig 12. Hourly total load and PV data for modified IEEE 118 bus

TABLE I
TOTAL PV INSTALLATION CAPACITIES AND THEIR LOCATIONS

Areas	Locations	Case 1	Case 2
A	bus 5, 11, 14, 16	176 MW	290 MW
B	bus 17, 20, 23, 29	174 MW	261 MW
C	bus 33, 35, 37, 41	145 MW	252 MW
D	bus 45, 48, 53, 67	126 MW	232 MW
E	bus 75, 83, 94, 98	101 MW	227 MW

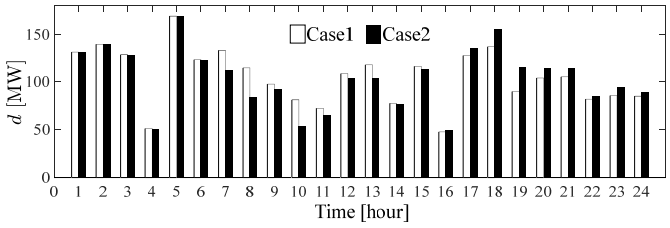

(a) $\sigma_{PV} = 0\%, \sigma_D = 3\%$

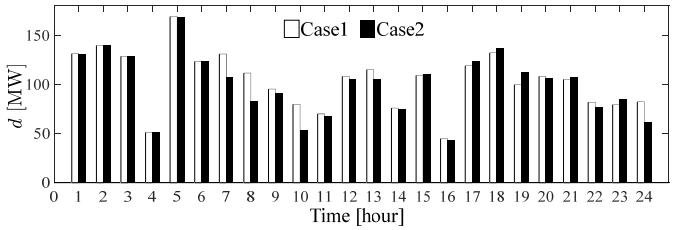

(b) $\sigma_{PV} = 10\%, \sigma_D = 3\%$

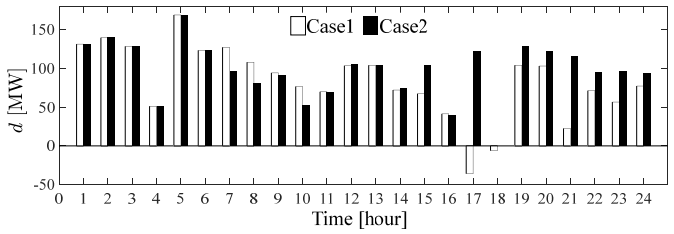

(c) $\sigma_{PV} = 30\%, \sigma_D = 3\%$

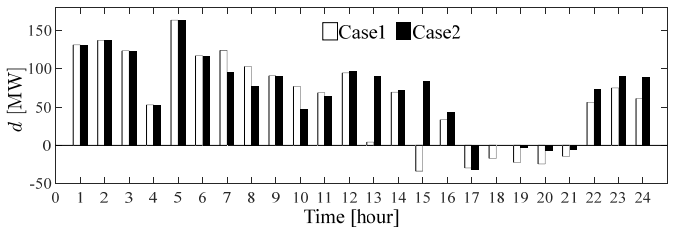

(d) $\sigma_{PV} = 30\%, \sigma_D = 3\%$ and N-1 contingency

Fig 13. Size of feasibility region d measured in MW; Negative values indicate possible power mismatch in the worst case.

one line at the line between buses 69 and 70, and that between bus 100 and 103. The characteristics of indicator d are similar to 6-bus system results. When the forecast is more erroneous, d is smaller, where the system operation may be less reliable and secure.

Negative d are observed at around 17:00, when the RDF region shrinks and disappears. When d is too small, the operator may take action in advance, such as obtaining additional power supply, demand response, load shedding etc. Such actions may be prepared in the system planning.

H. Computational Burden

CPU time for the proposed optimization method is listed in Table II. The simulations are carried out using Intel Core i7 2.20GHz, 8GB of RAM Memory. The proposed method is implemented using Matlab/Simulink optimization toolbox "intlinprog."

TABLE II
CPU TIME FOR OPTIMIZATION PROCESS

	Case	CPU Time (s) (Itlinprog)		CPU Time (s) (CPLEX)	
		6-bus	118-bus	6-bus	118-bus
σ_{PI}=0%, σ_D=3%	1	26.4	466.9	3.8	132.2
	2	26.9	516.3	3.6	122.2
σ_{PI}=10%, σ_D=3%	1	29.5	471.4	4.1	116.9
	2	29.0	493.1	4.5	119.2
σ_{PI}=30%, σ_D=3%	1	29.1	411.1	4.3	139.7
	2	28.9	542.2	4.5	122.1
σ_{PI}=30%, σ_D=3% with contingency	1	31.0	1.313	7.9	255.2
	2	32.0	2.437	8.4	239.8

We also use CPLEX [44] solver, which is about 10 times faster than "intlinprog" as listed in Table II. Since the present program is not optimized, improvement of the algorithm is necessary.

V. Transient Stability in West Japan System

A. Background

In West Japan Interconected System, transient stability (TS) is a critical factor limitting power transfer, while rapid increase in PV generations are causing uncertain power flows. The situation requires analysis of TS for possible uncertain power flows. The IEEJ West Japan standard model is used for this purpose, which is given in Fig. 14.

B. Analysis Method for Transient Stability

We propose the use of critical clearing time (CCT) as an index for TS. CCT is the critical value of fault clearing time for system stability. The reasons of using CCT as an index are: (1) CCT directly indicates the degree of TS; (2) CCT is useful for system control; (3) There are several options for the computation of CCT. The first option is the bisection method where conventional TS analysis tool is repeatedly used until required precision of CCT is obtained. The method is accurate but time consuming. The transient energy function methods are another options to obtain CCT. The methods are fast but

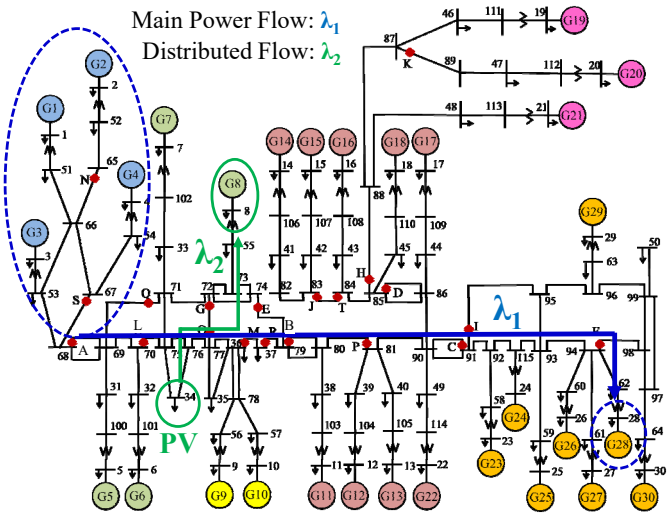

Fig. 14. IEEJ West Japan 30-Gen. Model (Total generation 100 GW).

TABLE III
CCT COMPUTATION PERFORMANCE OF CRITICAL TRAJECTORY METHOD

Fault Points	Exact Computation		CTrj Method			Error [%]
	CCT[s]	CPU[s]	CCT[s]	CPU[s]	Iter.	
A	0.084	1.002	0.083	0.223	27	-1.19
B	0.127	0.989	0.124	0.125	21	-2.36
C	0.113	0.979	0.113	0.130	22	0.00
D	0.151	0.985	0.150	0.102	19	-0.66
E	0.177	1.091	0.179	0.095	17	1.13
F	0.203	1.205	0.204	0.170	30	0.49
G	0.228	1.097	0.229	0.085	15	0.44
H	0.263	0.987	0.261	0.096	18	-0.76
I	0.347	1.320	0.346	0.074	13	-0.29
J	0.093	1.102	0.091	0.169	30	-2.15
K	0.128	1.108	0.125	0.127	22	-2.34
L	0.157	1.256	0.154	0.174	27	-1.91

errors are large.

In this paper, we use the critical trajectory (CTrj) method, which was proposed in [32]-[34] and has been improved to date. A monitoring and control method in terms of CCT will be proposed in the latter section using CTrj method. The computation performance of CTrj method is given in Table III.

C. TS Analysis in terms of CCT in West Japan System

We analyze TS using the west Japan system model in Fig. 14. We assume two kind of additional power flows, λ_1 and λ_2, to the original loading condition (100.2 GW loading). λ_1 implies additional main power flow from west to east, which is increased form 0 to 1.0 GW, while λ_2, local power flow caused by PV generation, is changed from 0 to 1.4 GW. Note that increase in λ_2 caused by PV generation is absorbed by generator G8, which makes the system light loading but unstable as is studied below.

We compute CCTs for various contingencies using bisection method, where we use the Xd' generator model with damping. The computed CCTs are given in Fig. 15(a), where λ_1 is changed from 0 to 1.0 GW with λ_2=0. It is observed that CCTs are decreased as additional power flow λ_1 is increased.

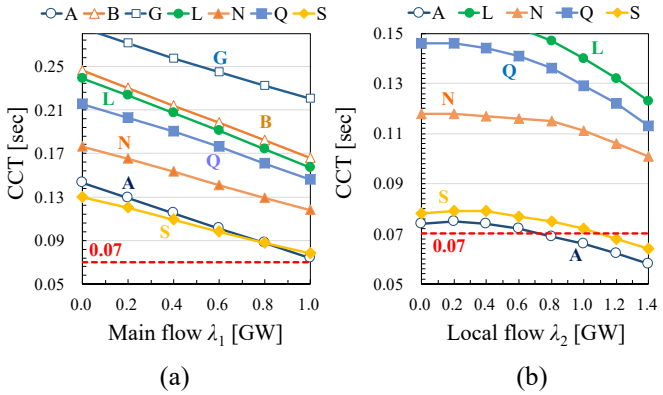

Fig. 15. TS Assessment in terms of CCT.

The system is still stable since all CCTs' are greater than the operation time of fault clearing relay, 0.07 [s]. Fig. 15(b) shows CCTs for variable λ_2 with fixed λ_1 =1.0 GW. The system becomes unstable for fault A when distributed power flow is deviated due to increase in PV output, λ_2 >0.8 GW. Note that fault S is also critical but can be stabilized together with fault A since they have the same characteristics.

From the above examination, it is observed that the increase in PV output may cause instability for TS. An important issue is that various patterns of such critical power flows for TS may exist caused by PV generations, and it is a fact that accurate PV outputs prediction is difficult. Therefore, an effective monitoring and control method is highly required.

VI. Monitoring and Control of Transient Stability

A. CCT Distribution Factor

Distribution factor (DisF) is widely used for power system control in order to avoid constraint violations such as overloadings of transmission lines, etc. We apply the same concept to the control of CCTs. We propose CCT-Distribution Factor (CCT-DisF) for contingency *n*, defined as:

TABLE IV
CCT-DISTRIBUTION FACTORS (λ_1= 1.0, λ_2=0.6)

Gen #	1	2	3	4	5	6	7	8	9	10
CCT-DisF	-0.07	-0.060	-0.070	-0.070	-0.040	-0.030	-0.030	-0.010	-0.010	-0.010
Gen #	11	12	13	14	15 slack	16	17	18	19	20
CCT-DisF	0.020	0.020	0.020	0.000	0.000	0.000	0.000	0.000	0.000	0.000
Gen #	21	22	23	24	25	26	27	28	29	30
CCT-DisF	0.000	0.000	0.000	0.000	0.000	0.000	0.000	0.000	0.000	0.000

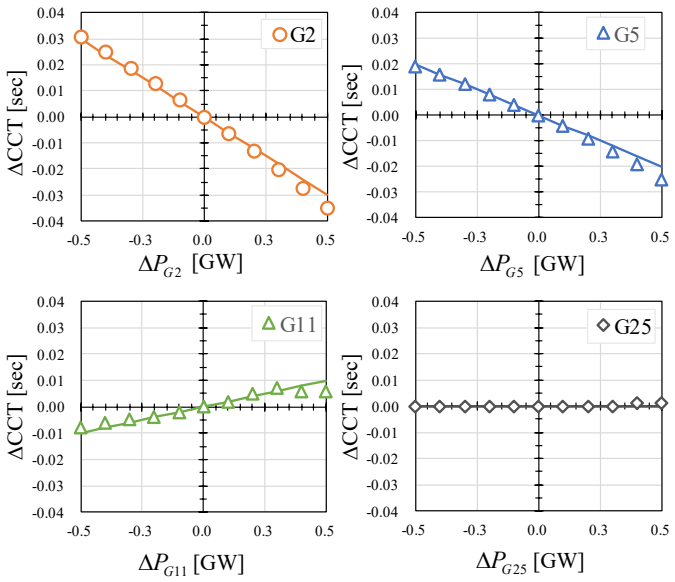

Fig. 16. Comparison of the estimated CCTs by CCT Distribution factors with the actual simulated values.

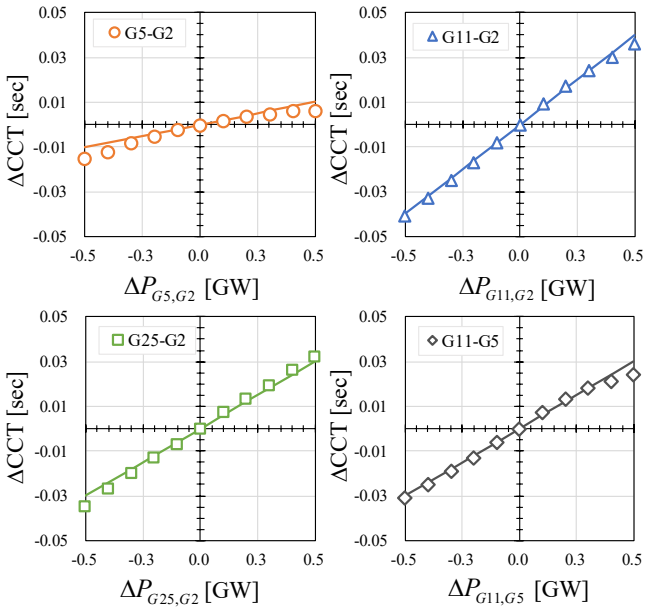

Fig. 17. Comparison of estimated and actual control effects.

$$CD_{Pj}^{(n)} = \frac{\Delta CCT^{(n)}}{\Delta P_j} \tag{31}$$

CCT-DisF implies the sensitivity of CCT with respect to power output of resouce *j* at prefault condition, P_j. The following numerical evaluation is suggested as a possible computation method at an operating point.

Step 1: Power flow computation with resetting $P_j = P_{j0} + \Delta P_j$ with prespecified deviation ($\Delta P_j = 0.1$), which is absorbed by slack generator.

Step 2: CCT computation by the CTrj method to obtain $\Delta CCT^{(n)}$ and $CD_{Pj}^{(n)}$.

We select an operating point at (λ_1 =1.0, λ_2 =0.6) and evaluate CCT-DisF for all generators *j* = G1 to G30 as given in Table IV, where G15 is the slack generator and the corresponding CCT-DisF is set to zero. Fig. 16 compares the estimated deviations of CCTs by CCT-DisF with the actual simulated values for several selected generators. As is observed, the errors in CCT-DisF are small enough to be used for TS control problem.

B. Preventive Control between Two Generators

We examine the use of CCT-DisF for the preventive control between two generators. We select two arbitrary generators, G*i* and G*j*, and assume relative control:

$$\Delta P_{Gi} = -\Delta P_{Gj} := \Delta P_{Gi,Gj} \tag{32}$$

The effect of the relative control is estimated by the difference of the corresponding CCT-DisFs as follows:

$$\Delta CCT^{(n)} = [CD_{PGi}^{(n)} - CD_{PGj}^{(n)}]\Delta P_{Gi,Gj} \tag{33}$$

Fig. 17 shows the Comparison of Estimated and Actual Control Effects. We see that, if there exists difference in the CCT-DisF, preventive control of TS is possible between the two generators.

C. Proposed Real-time Monitoring & Control for TS

We propose the following Monitoring and Control method for TS, where controllable resource outputs are represented as vector *u*, which may include P_j.
Repeat on-line:

Step 1: Load and RE forecast
Step 2: State Estimation
Step 3: Computation of CCT (CTrj method)
Step 4: Monitoring of TS constraint:

$$CCT > Thresh \quad .(34)$$

If TS constraint is violated for contingency *n*,
Step 5: Compute CCT-DisF (CTrj method)
Step 6: Determine ΔP to satisfy TS constraint:

$$CCT + CD_u^{(n)} \cdot \Delta u > Thresh \quad (35)$$

Step 7: Perform preventive control of ΔP.
ΔP may be optimally determined among possible controls.

VII. Robust Security Control for Transient Stability

A. Formulation

We propose a more reliable preventive control method for Step 7 in the previous section. The robust security formulation of (21) and (22) is applied to TS problem. Given an operating point, (u_0 , p_0) at which TS constraint (34) is violated ($CCT_0 < Thresh$), we assume that CCT-DisF has been computed and that a set of control resource is available as *u*. Then, based on the CCT-DisF, elements of *u* are divided into two groups so that any pair form each group can be used for relative control of (32).

$$\left.\begin{array}{l} u_i \geq u_{0i}, \quad i \in S_{UP} \\ u_i \leq u_{0i}, \quad i \in S_{Down} \end{array}\right\} \quad (36)$$

where u_{0i} is an operating point before control.

The classification of *u* may be performed to satisfy the following criteria based on (33):

$$CD_i^{(n)} - CD_j^{(n)} > 0, \quad i \in S_{UP}, \quad j \in S_{Down} \quad (37)$$

Node injection vector is represented in terms of controllable generators and uncertain parameters as:

$$\text{Node Injection: } = L_G u + L_p p + l_0 \quad (38)$$

$$u \in R^{N_G},\ p \in R^{Np},\ l_0 \in R^{N_B}$$

Then, we propose the following formulation, where TS constraint is additionally used.

Present operating point: (u_0 , p_0)
Control to be determined: *u*
PV generations in individual Areas (uncertainty)

$$R_p = \{p \mid \underline{p} \leq p \leq \overline{p}\} \quad (39)$$

Demand & Supply balance: $e^T \cdot (L_G u + L_p p + l_0) = 0$ (40)

TS constraint:

$$CCT_0 + CD_u^{(n)} \cdot (u - u_0) + CD_p^{(n)} \cdot (p - p_0) > Thresh \quad (41)$$

Line Flow Limit:

$$\underline{P}_{TL} \leq S^{(n)} \cdot (L_G u + L_p p + l_0) \leq \overline{P}_{TL} \quad n = 1 \ldots N \quad (42)$$

Controllable generator limits: $\underline{u} \leq u \leq \overline{u}$ (43)

Ramp rate limits: $-\delta \leq u - u_0 \leq \delta$ (44)

Finally, the following control cost is selected as an objective to form a liner bi-level optimization problem for a real-time preventive control:

$$\min_{u,p} \alpha = \sum_{i \in S_{UP}} c_i (u_i - u_{0i}) + \sum_{j \in S_{Down}} c_j (u_{0j} - u_j) \quad (45)$$

Subject to

$$Ap + Bu \leq b \quad (46)$$

$$u \in \arg\min_u \ \alpha \quad (47)$$

Subject to

$$Ap + Bu \leq b$$

In the above formulation, a set of linear constraints (46) consist of constraints (36), (39)-(44). The above problem is transformed into MILP problem.

We also examine the following objective that replace (45) with the same constraints.

$$\min_{u,p} \alpha = \sum_i c_i (u_i - u_{0i})^2 \quad (48)$$

The problem is transformed into MIQP problem. The above MILP and MIQP problems will be studied in the next section.

B. Examinations

We assume the operating point as is studied in section VI:

$$\lambda_1 = 1.0,\ \lambda_2 = 0.6,\ CCT_0 = 0.072 \quad (49)$$

We set the threshold of CCT in (34) as *Thresh* = 0.1. Then, we assume that incremental PV generations in three areas (p_1 for Kyushu at nodes 1-4, 51-54, p_2 for Chugoku at nodes 5-8, 31-35 and 55, p_3 for the other areas) are regarded as uncertain parameters, whose predictions and CIs are set as:

$\hat{p}_1 = 0.05$, $[\underline{p}_1, \overline{p}_1] = [0, 0.1]$ [GW]

$\hat{p}_2 = 0.05$, $[\underline{p}_2, \overline{p}_2] = [0, 0.1]$ [GW]

$\hat{p}_3 = 0.05$, $[\underline{p}_3, \overline{p}_3] = [0.05, 0.05]$ [GW]

CCT-DisF for uncertain parameters are computed in the same way as given in section VI. A, which are used for constraints (41) with the CCT-DisF in Table IV.

We first examine the following four cases of optimizations for preventive control using the linear objective (45):

- Method A (LP): The deterministic minimization with (46) and $p = \hat{p}$.
- Method B (MILP): The worst-case minimization with (46)-(47) and uncertainty (39). This case corresponds to $\underline{\alpha}_{RDF}(t=1)$ in (22).
- Method C (MILP): The worst-case maximization with (46)-(47) and uncertainty (39), corresponding to $\overline{\alpha}_{RDF}(t=1)$ in (23). This case is for the evaluation of the region size of RDF.
- Method D (LP): The deterministic maximization with (46) using $p = \hat{p}$, This case is just for reference.

Table V lists the CCTs and control costs for the above four cases with the objective (45) with c_i = 1. We first compare "Designed" CCTs, which implies the results by Method A and by Method B. The designed CCTs by Method B always satisfies TS constraint (CCT>0.1) since it is designed for the worst prediction error case. On the other hand, CCT by Method A is acceptable when the PV prediction is accurate with no errors; if prediction errors are present, CCT may violate its threshold as seen in the worst case of PV prediction errors.

"Actual" CCT in the Table implies the CCT obtained after the preventive control. We see that there exist small errors in the proposed controls of Methods A and B due to the linearization errors in CCT-DisF.

TABLE V
IMPROVED CCTS BY PREVENTIVE TS CONTROLS
LINEAR OBJECTIVE CASES

Control Method	CCTs (Thresh=0.1)		Control Cost (α)
	Designed	Actual	
Method A (LP)			
-No prediction error	0.1000	0.0985	0.6222
-Worst-case error	0.0985	0.0966	
Method B (MILP)			
-No prediction error	0.1015	0.1003	0.6976
-Worst-case error	0.1000	0.0984	
Method C (MILP)	-	-	23.0848
Method D (LP)	-	-	23.1600

TABLE VI
IMPROVED CCTS BY PREVENTIVE TS CONTROLS
QUADRATIC OBJECTIVE CASES

Control Method	CCTs (Thresh=0.1)		Control Cost (α)
	Designed	Actual	
Method A (QP)			
-No prediction error	0.1000	0.1009	0.0411
-Worst-case error	0.0985	0.0992	
Method B (MIQP)			
-No prediction error	0.1015	0.1041	0.0489
-Worst-case error	0.1000	0.1024	
Method C (MIQP)	-	-	16.8172
Method D (QP)	-	-	16.8343

Table V also compares the control costs for methods A to D, which correspond to four types of bounds given in Fig. 4. We can observe the followings:

$$\alpha^{Method\ A} < \alpha^{Method\ B} < \alpha^{Method\ C} < \alpha^{Method\ D} \tag{50}$$

The first and the last inequalities always hold since the worst-case minimum and maximum by Method B and Method C respectively provide the upper bound of minimums and the lower bound of maximums among uncertainties. On the other hand, the second inequality is not the case as is investigated in the previous section. Distance d measured by the following equation implies the size of feasible region, which may be inverted when the region disappears.

$$d = \alpha^{Case\ C} - \alpha^{Case\ B} \tag{51}$$

A positive d guarantees the feasibility for the preventive controls. A negative d implies the nonexistence of operating points satisfying the constraints in the worst case, implying that even the control designed by Method B cannot be guaranteed.

Next, the linear objective (45) is replaced by quadratic objective (48) with setting c_i = 1. The quadratic objective is more flexible since we can avoid a preliminary classification of control groups such as (36). This seems advantageous when we face a situation where multiple critical contingencies appear. Then, using (48), we have four quadratic programming (QP) problems with the same conditions as before, corresponding to Methods A to D. Table VI shows the results of the optimizations. As we have expected, very similar results are obtained, where we can state exactly the same discussions as before.

We finally suggest that three methods A to C are effectively used for monitoring and control. Method A may be used for a control target assuming that the prediction is exact enough. For unreliable predictions, method B is useful to obtain reliable safe-side control under uncertainty. We can use Method C to monitor the size of the feasible region, *d,* as well as the reliability of the control by Method B. We suggest a combined use of methods A to C for economic and reliable power system operations satisfying Robust Power System Security.

VIII. Conclusion

This paper proposes a new method to compute the size of the worst-case feasible region under uncertainties. The method utilize predictions of uncertain parameters including the bounds of prediction errors which are set based on confidence intervals (CIs). The proposed method computes the security region size defined in the controllable parameter space by specifying CIs. The formulation allows various settings of uncertainties to check if the conventional deterministic power system security criterion suffices in the system planning and operation. The proposed approach is useful for the evaluation

of the robust power system security, which is the worst-case security assessment against uncertainties.

Dynamic economic dispatch problem with uncertainties of PV forecast is investigated, where the security assessment of 24-hour system operation is carried out. It has been confirmed that the method is useful to analyze the feasibility of system operation, the degree of system reliability against uncertainties.

The latter half of the paper investigates transient stability (TS) in West Japan System and shows that PV generations may cause various power flows where TS is critical. This implies that effective monitoring method will be required in the future.

We propose a monitoring and control method for TS using critical clearing time (CCT) based on the critical trajectory method. We also suggest the use of the sensitivity of CCT to generator outputs for a preventive control of TS, which is referred to as CCT-Distribution Factor (CCT-DisF) in this paper.

CCT-DisF is applied to the generation dispatch problem to formulate a bi-level optimization for real-time preventive control problem with uncertainties.

Future Works

The proposed bi-level optimization method cannot be applied to a large system due to computational burden at present. Improvement of the algorithm or application of faster solution methods will be expected in the future.

The solution method we use at present is the most common approach based on Karush-Kuhn-Tucker (KKT) optimality condition given in the Appendix. However, reference [39] suggests the use of alternative approach based on primal-dual transformation from the point of view of computational efficiency. The application of the method seems effective to decrease number of binary variables.

Other necessary examinations include effective treatment of N-k contingencies such as tighter treatment of security criteria in [7]–[9], [14], [15]. Improvement of computational techniques concerned with contingencies are important subject.

Application of faster solution such as decomposition method is expected to solve the problem for a large scale system.

IX. Appendix

A. Solution of Region Size Problem for RSS

Original problem (21) after linearization may be rewritten as the linear bi-level optimization problem as follows.

$$\bar{\alpha}_{RSS} = \min_{u,p}\{c^T u\} \tag{A.1}$$

Subject to

$$Ap + Bu \le b \tag{A.2}$$

$$u \in \arg\max_{u}\left\{c^T u\right\} \tag{A.3}$$

Subject to

$$Ap + Bu \le b \tag{A.4}$$

The lower-level problem (A.3)-(A.4) is transformed by using KKT necessary optimality condition into a set of constraints in the upper level problem to form a single-level problem. A binary vector and sufficiently large value L are introduced to treat the non-linear complementary slackness condition to obtain its equivalent linear form. Thus, the original bi-level problem (A.1)-(A.4) is converted into an equivalent single-level optimization problem (A.5)-(A.11). The complete derivation is given in [45].

$$\bar{\alpha}_{RSS} = \min_{u,p}\{c^T u\} \tag{A.5}$$

Subject to

$$Ap + Bu \le b \tag{A.6}$$

$$\begin{bmatrix} u^T & \lambda^T \end{bmatrix} \le L\begin{bmatrix} u_{bin}^T & \lambda_{bin}^T \end{bmatrix} \tag{A.7}$$

$$\begin{bmatrix} c - A^T\lambda \\ b - Bu - Ap \end{bmatrix} \le L\begin{bmatrix} 1-u_{bin} \\ 1-\lambda_{bin} \end{bmatrix} \tag{A.8}$$

$$c^T \le \lambda^T A \tag{A.9}$$

$$\lambda \ge 0 \tag{A.10}$$

$$u_{bin}, \lambda_{bin} \in \{0,1\} \tag{A.11}$$

L: Large value (L=50,000 is used.)

The similar procedure may be applied to problem (22) to obtain the equivalent problem as follows:

$$\underline{\alpha}_{RSS} = \max_{u,p}\{c^T u\} \tag{A.12}$$

Subject to constraints (A.6)-(A.11).

The obtained MILP can be solved by a commercial software package such as MATLAB/SIMULINK Optimization Toolbox.

X. References

[1] T. E. Dy Liacco, "System security: the computer's role," *IEEE Spectrum*, vol. 15, no. 6, pp. 43-50, Jun. 1978.

[2] B. Stott and E. Hobson, "Power system security control calculations using linear programming, Part1&2," *IEEE Trans. Power App. Syst*., vol. PAS-97, no. 5, pp. 1713-1731, Sep./Oct. 1978.

[3] M. H. Banakar and F. D. Galiana, "Power system security corridors concept and computation," *IEEE Trans. Power App. Syst*., vol. PAS-100, no. 11, pp. 4524-4532, Nov. 1981.

[4] B. Stott and J.L. Marinho, "Linear programming for power-system network security applications," *IEEE Trans. Power App. Syst.*, vol. PAS-98, no. 3, pp. 837-848, May/Jun. 1979.

[5] J. L. Carpentier and G. Cotto, "Modern concepts for security control in electric power system," No. R-102-01, in *Proc. of CIGRE-IFAC Symp. on Control Applications to Power System Security*, Florence, Italy, Sep. 1983.

[6] B. Stott, O. Alsac, and A.J. Monticelli, "Security analysis and optimization," in *Proc. of the IEEE*, Dec. 1987, pp. 1623-1644.

[7] A. L. Motto, J. M. Arroyo, and F. D. Galiana, "A mixed integer LP procedure for the analysis of electric grid security under disruptive threat," *IEEE Trans. Power Syst.*, vol. 20, no. 3, pp. 1357-1365, Aug. 2005.

[8] J. M. Arroyo, and F. D. Galiana, "On the solution of the bilevel programming formulation of the terrorist threat problem," *IEEE Trans. Power Syst*., vol. 20, no. 2, pp. 789–797, May 2005.

[9] J. Salmeron, K. Wood, and R. Baldick, "Worst-case interdiction analysis of large-scale electric power grids," *IEEE Trans. Power Syst*., vol. 24, no. 1, pp. 96–103, Feb. 2009.

[10] T. Kim, S. J. Wright, D. Bienstock, and S. Harnett, "Analyzing vulnerability of power systems with continuous optimization formulations", *IEEE Trans. Power Syst*., vol. 3, no. 3, pp. 132–146, Sept. 2016.

[11] S. Fliscounakis, P. Panciatici, F. Capitanescu, and L. Wehenkel, "Contingency ranking with respect to overloads in very large power systems taking into account uncertainty, preventive and corrective actions," *IEEE Trans. Power Syst.*, vol. 28, no. 4, pp. 4909-4917, Nov. 2013.

[12] Y. Yuan, J. Kubokawa, and H. Sasaki, "A solution of optimal power flow with multicontingency transient stability constraints," *IEEE Trans. Power Syst*., vol. 18, no. 3, pp. 1094-1102, Aug. 2003.

[13] Q. Wang, J. D. McCalley, T. Zheng, and E. Litvinov, "A computational strategy to solve preventive risk-based security-constrained opf," *IEEE Trans. on Power Syst*., vol. 28, no. 2, pp. 1094-1102, May 2013.

[14] A. Street, F. Oliveira, and J. M. Arroyo, "Contingency-constrained unit commitment with *n-k* security criterion: A robust optimization approach," *IEEE Trans. Power Syst.*, vol. 26, no. 3, pp. 1581-1590, Aug. 2011.

[15] A. Moreira, A. Street, and J. M. Arroyo, "An adjustable robust optimization approach for contingency-constrained transmission expansion planning," *IEEE Trans. Power Syst*., vol. 30, no. 4, pp. 2013–2022, Jul. 2015.

[16] N. Yorino, E. E. El-Araby, H. Sasaki, and S. Harada, "A new formulation for FACTS allocation for security enhancement against voltage collapse," *IEEE Trans. Power Syst*., vol. 18, no. 1, pp. 3-10, Feb. 2003.

[17] D. Bertsimas, E. Litvinov, X. A. Sun, J. Zhao, and T. Zheng, "Adaptive robust optimization for the security constrained unit commitment problem," *IEEE Trans. Power Syst*., vol. 28, no. 1, pp. 52-63, Feb. 2013.

[18] A. Lorca, and X. A. Sun, "Adaptive robust optimization with dynamic uncertainty sets for multi-period economic dispatch under significant wind," *IEEE Trans. Power Syst*., vol. 30, no. 4, pp. 1702–1713, Jul. 2015.

[19] F. Capitanescu, S. Fliscounakis, P. Panciatici, and L. Wehenkel, "Cautious operation planning under uncertainties," *IEEE Trans. Power Syst.*, vol. 27, no. 4, pp. 1859-1869, Nov. 2012.

[20] F. Capitanescu and L. Wehenkel, "Computation of worst operation scenarios under uncertainty of static security management," *IEEE Trans. Power Syst.*, vol. 28, no. 2, pp. 1697-1705, May 2013.

[21] J. Warrington, C. Hohl, P. J. Goulart, and M. Morari, "Rolling unit commitment and dispatch with multi-stage recourse policies for heterogeneous devices," *IEEE Trans. Power Syst.*, vol. 31, no. 1, pp. 187-197, Nov. 2016.

[22] O. Alizadeh-Mousavi and M. Nick A, "Stochastic security constrained unit commitment with variable-speed pumped-storage hydropower plants," in *Proc. of 19th Power System Computation Conference (PSCC)*, Jun. 2016, pp.1-6.

[23] E. Lannoye, D. Flynn, and M. O'Malley, "Evaluation of power system flexibility," *IEEE Trans. Power Syst.*, vol. 27, no. 2, pp. 922-931, May 2012.

[24] J. Zhao, T. Zheng, and E. Litvinov, "A unified framework for defining and measuring flexibility in power system," *IEEE Trans. Power Syst*., vol. 31, no. 1, pp. 339-347, Jan. 2016.

[25] M. A. Bucher, S. Chatzivasileiadis, and G. Andersson "Managing flexibility in multi-area power systems," *IEEE Trans. Power Syst*., vol. 31, no. 2, pp. 1218–1226, Mar. 2016.

[26] J. Zhao, T. Zheng, and E. Litvinov, "Variable resource dispatch through do-not-exceed limit," *IEEE Trans. Power Syst*., vol. 30, no. 2, pp. 820–828, Mar. 2015.

[27] A. S. Korad and K. W. Hedman, "Enhancement of do-not-exceed limit with robust corrective topology control," *IEEE Trans. Power Syst*., vol. 31, no. 3, pp. 1889–1899, May 2016.

[28] W. Wei, F. Liu, and S. Mei, "Dispatchable region of the variable wind generation," *IEEE Trans. Power Syst*., vol. 30, no. 5, pp. 2755–2765, Sept. 2015.

[29] A. A. Jahromi and F. Bouffard, "On the loadability sets of power systems–Part I: Characterization, &–Part II: Minimal Representations," *IEEE Trans. Power Syst*., vol. 32, no. 1, pp. 137-156, Jan. 2017.

[30] Y. Okumoto, N. Yorino, Y. Zoka, Y. Sasaki, T. Yamanaka, and T. Akiyoshi, "An application of robust power system security to power system operation for high-penetration of PV," in *Proc. of IEEE PES Innovative Smart Grid Technologies Conf.*, Oct. 2012, pp. 1-7.

[31] N. Yorino, Y. Sasaki, E.P. Hristov, Y. Zoka, and Y. Okumoto, "Dynamic load dispatch for power system robust security against uncertainties," in *Proc. of 2013 IREP Symp.*, Crete, Greece, Aug. 2013, pp. 1-17.

[32] N. Yorino, E. Popov, Y. Zoka, Y. Sasaki, and H. Sugihara, "An application of critical trajectory method to bcu problem for transient stability studies," *IEEE Trans Power Syst.*, vol. 28, no. 4, pp. 4237-4244, Nov. 2013.

[33] N. Yorino, A. Priyadi, H. Kakui, and M. Takeshita, "A new method for obtaining critical clearing time for transient stability," *IEEE Trans. Power Syst.*, vol. 25, no. 3, pp. 1620-1626, Aug. 2010.

[34] A. Priyadi, N. Yorino, M. Tanaka, T. Fujiwara, H. Kakui, and M. Takeshita, "A direct method for obtaining critical clearing time for transient stability using critical generator conditions," *European Trans. on Electrical Power*, vol. 22, no. 5, pp. 674-687, Jul. 2012.

[35] N. Yorino, M. Abdillah, T. Isoya, Y. Sasaki, and Y. Zoka, "A new method of evaluating robust power system security against uncertainties," *IEEJ Trans. on Elect.and Electron.Eng.*, vol. 10, no. 6, pp. 636-643, Nov. 2015.

[36] Y. Sasaki, N. Yorino, and Y. Zoka, "Probabilistic economic load dispatch applied to a micro-ems controller," in *Proc. of 19th Power System Computation Conference (PSCC)*, Jun. 2016, pp.1-6.

[37] H.M. Hafiz, N. Yorino, Y. Sasaki, and Y. Zoka, "Feasible operation region for dynamic economic dispatch and reserve monitoring," *European Trans. on Electrical Power*, vol. 22, no. 7, pp. 924-936, Oct. 2012.

[38] N. Yorino, H. M. Hafiz, Y. Sasaki, and Y. Zoka, "High-speed real-time dynamic economic load dispatch," *IEEE Trans. Power Syst.*, vol. 27, no. 2, pp. 621-630, May 2012.

[39] J. M. Arroyo. "Bilevel programming applied to power system vulnerability analysis under multiple contingencies," *IET Generation, Transmission & Distribution*, vol. 4, no. 2, pp. 178-190, Feb. 2010.

[40] H. Wu, M. Shahidehpour, and M.E. Khodayar, "Hourly demand response in day-ahead scheduling considering generating unit ramping cost", *IEEE Trans. Power Syst.*, vol. 28, no. 3, pp. 2446-2454, Aug. 2013.

[41] H. Wu, X. Guan, Q. Zhai, F. Gao, and Y. Yang, "Security-constrained generation scheduling with feasible energy delivery," in *Proc. 2009 IEEE Power Eng. Soc. General Meeting*, Calgary, AB, Canada, Jul. 2009, pp.1-6.

[42] National renewable energy laboratory (NREL), data and resources [Online]. Available:http://www.nrel.gov/electricity/transmission/data_resources.html.

[43] IEEE 118-Bus System, llinois institute of technology [Online]. Available: motor.ece.iit.edu/data.

[44] IBM ILOG CPLEX optimization studio [Online]. Available:https://www-01.ibm.com/software/commerce/optimization/cplex-optimizer.

[45] C. Audet, P. Hansen, B. Jaumard, and G. Savard, "Links between linear bilevel and mixed 0–1 programming problems," *Journal of Optimization Theory and Applications*, vol. 93, no. 2, pp. 273-300, May 1997.